

¹⁷ D. Jerome, Ch. Ryter, and J. M. Winter, *Physics* **2**, 81 (1965).

¹⁸ D. A. Zhogolev, *Fiz. Tverd. Tela* **9**, 59 (1967) [*Soviet Phys. Solid State* **9**, 42 (1967)].

¹⁹ Z. M. Jarzebski, *Acta Phys. Polon.* **29**, 37 (1966).

²⁰ J. C. Phillips and J. A. Van Vechten, *Phys. Rev. Letters* **22**, 705 (1969).

²¹ E. H. Putley, *The Hall Effect and Related Phenomena* (Butterworths, London, 1960), p. 42ff.

²² J. M. Ziman, *Electrons and Phonons* (Clarendon, London, 1960), Chap. 10.

²³ R. P. Khosla and J. R. Fischer, *Bull. Am. Phys. Soc.* **15**, 316 (1960).

²⁴ A tabulation and discussion of the properties of CdO may be found in M. Neuberger, *Cadmium Oxide Data Sheet DS-149*, 1966 (unpublished). Copies may be obtained from DDC, Cameron Station, Bldg. 5, 5010 Duke St., Alexandria, Va. 22314.

²⁵ V. K. Miloslavskii and A. I. Ranyuk, *Opt. i Spectroskopiya* **11**, 289 (1961).

²⁶ Y. Toyozawa, *J. Phys. Soc. Japan* **17**, 980 (1962).

²⁷ N. Mikoshiba, *Rev. Mod. Phys.* **40**, 833 (1968).

Luminescence of Donor-Acceptor Pairs in Cubic SiC

W. J. CHOYKE AND LYLE PATRICK

Westinghouse Research Laboratories, Pittsburgh, Pennsylvania 15235

(Received 1 July 1970)

The photoluminescence of donor-acceptor pairs, under laser excitation, was recorded at 1.8°K. The spectrum is type II, and is attributed to N-Al pairs. Well-resolved lines were identified up to the 80th shell, and the van der Waals and multipole interactions were evaluated, following procedures used for the very similar GaP pair spectra. The limiting photon energy for distant pairs is $h\nu_{\infty} = 2.0934$ eV. As in some GaP spectra, intensity anomalies were observed. With the GaP work serving as a guide, one intensity anomaly was interpreted as a channel cutoff, another as a phonon resonance. This permitted us to evaluate the ionization energies, $E_D = 118$ meV for N, and $E_A = (179 \text{ meV}) + E_x$ for Al, with E_x the still unknown exciton binding energy. With lower resolution the maximum and the half-width of the spectrum envelope were measured as a function of excitation intensity, and phonon replicas were recorded. The band maximum at low excitation yields an impurity level of $1.6 \times 10^{18} \text{ cm}^{-3}$.

I. INTRODUCTION

The low-temperature luminescence of donor-acceptor (DA) pairs yields a spectrum rich in narrow lines.¹ DA pairs in GaP provide the best and most numerous examples. The early GaP spectra gave information on donor and acceptor ionization energies,² and on the van der Waals interaction between neutral donors and acceptors.³ Improvements in crystal growth and in experimental techniques yielded spectra of high quality that permitted a more detailed analysis.^{4,5} These spectra provided information on the multipole moments of the ions,⁶ and some details of the double-capture process that precedes light emission.⁷

The SiC spectrum we show here was first observed in 1963, and attributed to N-Al pairs,⁸ but it appeared impossible to give a satisfactory analysis at that time. We now use laser excitation to obtain a spectrum comparable in quality to some of the GaP spectra, and we can use the experience gained in GaP to analyze it fully. Cubic SiC and GaP have the same crystal structure (zinc-blende), hence the same shell structure for DA pairs.

In Sec. II terms are defined, and theoretical relationships are summarized. The experimental results are shown in Sec. III. Our fitting of the spectrum is then discussed in Sec. IV. The interpretation of two intensity anomalies permits us to break down into separate parts

the value deduced for the sum of the ionization energies, $E_D + E_A$. We discuss the multipole terms, and the difficulties encountered in fitting close pairs. Our conclusions are summarized in Sec. V.

II. THEORETICAL RELATIONSHIPS

The lines of a DA pair spectrum are fitted to the formula first given by Hopfield *et al.*,¹

$$h\nu = E_g - (E_D + E_A) - E_C + E_{vdw}, \quad (1)$$

where E_g is the energy gap, E_D and E_A are the donor and acceptor ionization energies, E_C is the Coulomb interaction energy between donor and acceptor ions *after* electron-hole recombination, and E_{vdw} is the interaction energy between neutral donor and acceptor atoms *before* recombination.

At first it was assumed that $E_C = -e^2/\epsilon r$, where ϵ is the static dielectric constant and r is the DA separation, which takes on the set of discrete values permitted by the lattice structure. Thus, for a given donor, a value of E_C was calculated for each shell of equidistant acceptors, the shells being denoted by the integers m . However, for nearest neighbors (small m) it was observed that spectral lines had to be assigned to each crystallographically inequivalent set of a given shell. It is now possible to account for the shell *substructure* by including multipole terms in E_C , for these terms have a dependence on both the DA separation and lattice direction.⁶

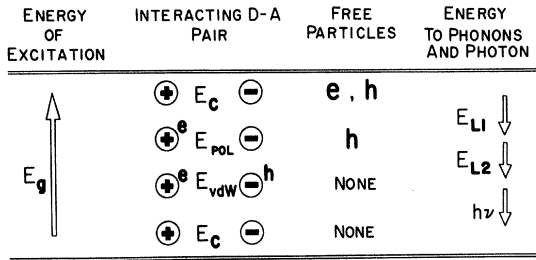


FIG. 1. Schematic of excitation-recombination cycle, using the e - h capture channel. From top to bottom the four rows represent successive stages during the cycle. The arrows indicate energy-changing steps, excitation being one step and recombination three. Circled charges are the donor and acceptor ions, and the DA interaction energy is shown for each stage of the cycle. This figure serves as a definition of E_C , E_{pol} , and E_{vdW} .

The term E_{vdW} is found to have the expected r^{-6} dependence of a van der Waals interaction for large m (i.e., large r). For small m , however, other interactions are important and the r^{-6} dependence fails. Nevertheless, E_{vdW} is defined as the total interaction energy between neutral donor and acceptor, and we determine its value at small m from the measured photon energy and Eq. (1).

Photon emission by DA pairs is preceded by a two-step capture event in which the energy E_{L1} is given to the lattice in the first capture step, and the energy E_{L2} in the second. The electron and hole may be captured in either order (for large m) and we use the notation " e - h " for electron-first capture, and " h - e " for hole-first capture. Figure 1 illustrates the energy balance in the excitation-recombination cycle (through the e - h capture channel) and it serves to define the interaction energies E_C , E_{vdW} , and E_{pol} . Note that E_{pol} is thereby defined as the total interaction energy between an ion and a neutral atom. Only for large m do we expect E_{pol} to be proportional to r^{-4} .⁷ A similar broad definition of E_{vdW} was stated above.

From Fig. 1 we can write down the relations

$$E_{L1} = E_D + E_C - E_{pol}, \quad (2)$$

$$E_{L2} = E_A + E_{pol} - E_{vdW}. \quad (3)$$

For the h - e capture channel E_D and E_A would be interchanged in Eq. (2) and (3). Note that E_C , E_{pol} , and E_{vdW} are all negative quantities, the three interactions all being attractive. Equations (2) and (3) were given in Ref. 7, where they proved useful in explaining several intensity anomalies in GaP pair spectra.

The intensity anomalies, observed under low excitation, result from changes in capture modes. A capture cutoff occurs at an m for which E_{L1} approaches zero, for energy must be dissipated to the lattice in capture.^{9,10} A capture resonance occurs when the energy given up in a capture step, say E_{L2} , is equal to the TO or LO phonon energy, for then the capture requires only the emission of a single phonon. Both kinds of intensity

anomaly are observed in the DA pair spectrum reported here. They are similar to the GaP intensity anomalies in magnitude, and our interpretation parallels that used for GaP in Ref. 7.

III. EXPERIMENTAL

We have observed only one DA spectrum in cubic SiC. Our identification of the donor as N and the acceptor as Al is tentative, and is based on the evidence given in Sec. III A. The sharp spectral lines are shown in Sec. III B and are identified by shell number, using Eq. (1) and the methods long employed for determining shell numbers in GaP spectra. Under different experimental conditions, as shown in Sec. III C, the same DA spectrum may be viewed as a band spectrum with phonon replicas. In this form it was previously reported by Zanmarchi,¹¹ but he observed it only in the presence of a second interfering band system.

A. Crystal Growth

Our cubic SiC samples were grown from the vapor in a furnace¹² also used to grow $6H$ and other SiC polytypes. Although cubic SiC grows at a lower temperature, many furnace runs provided both $6H$ and cubic samples, the latter probably being grown as the furnace cooled. In such cases the impurities in the cubic SiC are expected to be the same as in the $6H$ SiC, for which the effects of doping with N and Al are known.

In $6H$ SiC and other polytypes, N alone gives a bound-exciton spectrum at low temperatures,¹³ and when Al is added a strong DA pair spectrum appears. These two spectra predominate in the crystals grown in our laboratories, and their relationship to N and Al has been well established for the common $6H$ polytype. The spectra change with polytype, of course, but the characteristics of bound-exciton and DA spectra remain. Each spectrum was observed in cubic SiC crystals grown in the same furnace run with $6H$ crystals having the corresponding $6H$ spectrum. The cubic SiC bound-exciton spectrum was reported earlier,^{8,14} and the DA spectrum is the one shown here. In view of the above, we attribute it to N-Al pairs. We have observed no other DA spectrum in cubic SiC.

B. Line Spectrum

Our cubic SiC specimens were selected for DA luminescence, but high excitation usually brought out strong N bound-exciton luminescence also. The low excitation intensity needed to favor the DA spectrum was obtained by using a defocused beam of penetrating light. The 4880-Å line of an Ar ion laser is very suitable, for the absorption constant at 2.54 eV is only 25 cm⁻¹. The luminescence was orange under these conditions. A focused beam brought out the green bound-exciton luminescence and also many thermally excited lines of the DA spectrum, even though the samples were immersed in He at 1.8°K.

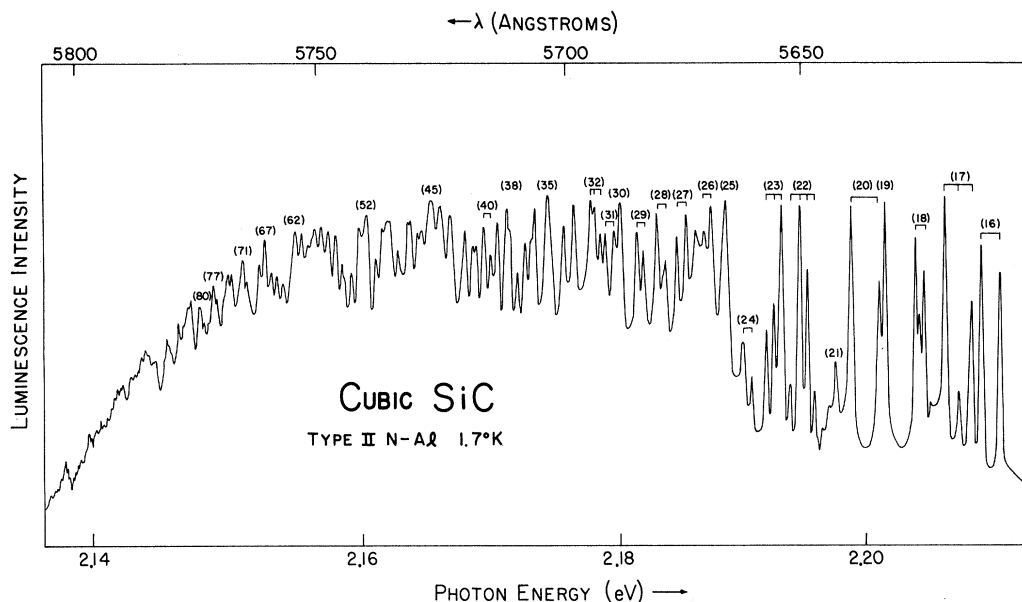


FIG. 2. Spectral lines for $m \geq 16$. Shell numbers are shown in brackets, and shell substructure components are identified for small m , where they are well resolved.

Figure 2 shows a densitometer trace of the DA pair spectrum for $m \geq 16$, and Fig. 3 shows the region $m \leq 20$. The spectra were photographed on Kodak 103F plates, using a Spex 1400 monochromator in second order. Filters were used to discriminate against the strong luminescence at large m , which will be shown in its true proportion in Sec. III C.

The spectrum was recognized as type II, and the lines

were identified by shell numbers up to $m=80$. Some of these numbers are shown, with resolved components joined by braces. Most of the substructure is resolved¹⁵ to $m \approx 32$. The spectrum appears to be very nearly free of extraneous lines.¹⁶ For small m the multipole splittings are large enough to result in some overlap of adjacent shells (e.g., $m=7$ and 8).

The number of equivalent DA pairs⁶ contributing to

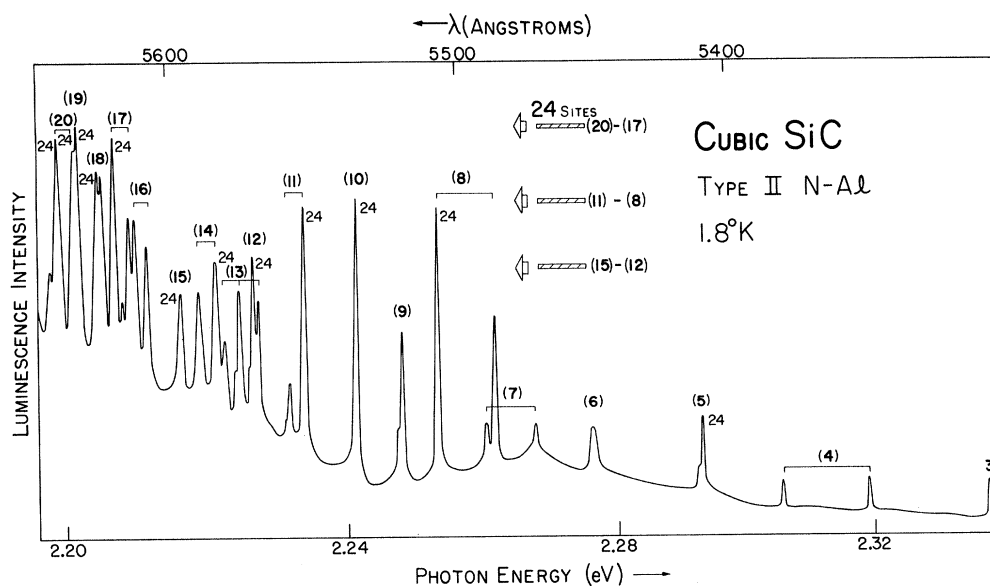


FIG. 3. Spectral lines for $m \leq 20$. The notation is like that of Fig. 2, except that all lines due to 24 equivalent pairs are marked. Intensity levels for groups of these lines are shown, indicating where the intensity anomalies appear.

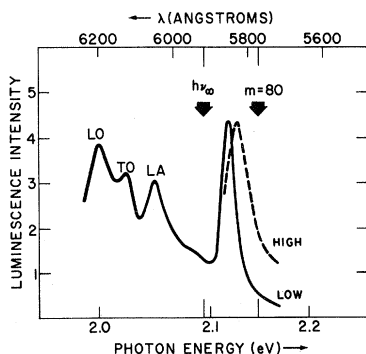


FIG. 4. The low-resolution envelope of the DA spectrum (largest peak), with phonon replicas (LA, TO, and LO). The solid and broken lines are measured under low and high excitation, respectively. The relationship to Fig. 2 is indicated by the position of the unresolved $m=80$ line. The limiting photon energy for distant pairs is $h\nu_\infty=2.0934$ eV.

a resolved line is 4, 12, or 24. The usual intensity rule, used as a guide in line identification, is "equal intensities per donor-acceptor pair" for nearby lines. Two strong violations of this rule are observed in Fig. 3, where lines due to 24 equivalent pairs are marked. It is assumed that these violations indicate changes in capture mode.⁷

C. Band Spectrum

The line spectrum of Figs. 2 and 3 is only the high-energy tail of a broad spectrum with phonon replicas. For Fig. 4 low resolving power (≈ 5 Å) was used, so that we recorded only the envelope of the multiline spectrum (lines for $m > 80$ were not well resolved even in Fig. 2). In addition, the range was extended to energies less than $h\nu_\infty$, where phonon emission is necessary for the existence of a DA spectrum. Photoelectric detection was used, and the measured intensity was corrected for the response of the optical system.

As previously reported for DA spectra in GaP,² increased excitation broadens the bands and displaces them toward higher energy, because of the saturation of distant pairs. For low excitation (solid curve) a defocused Hg arc was used, from which the strongly absorbed short wavelengths were filtered. For high excitation (broken curve) focused short-wavelength light was used, which probably increased the excitation intensity by a factor 50 or more. Only the no-phonon band is shown for high excitation, and it is normalized at the peak in Fig. 4 for easy observation of the shift and broadening. The shell number corresponding to the peak of the no-phonon band changed from $m \approx 360$ to $m \approx 210$ under the increased excitation intensity.

The phonon replicas are displaced from the no-phonon peak by approximately 69, 94, and 118 meV, corresponding to LA, TO, and LO phonons. There appears to be a large contribution to the LO band from zone-center phonons, the LO phonon energy being

120.5 meV at the center,¹⁷ and 103 meV at X .⁸ Some weaker two-phonon bands were observed, but are not shown in Fig. 4.

Zanmarchi observed the DA band spectrum, which he called "B," in crystals in which he could not resolve the line spectrum.¹¹ His samples also had another spectrum, which he called "A," that prevented him from detecting the TO phonon band of the DA spectrum. We have also observed the A spectrum in some samples at 77°K, but we do not know its origin. Zanmarchi attributed the A spectrum to Al, but we shall give evidence against this assignment.

IV. INTERPRETATION AND DISCUSSION

Similarities in the DA pair spectra of cubic SiC and GaP are not unexpected. Both materials have the zinc-blende structure. The cubic SiC energy gap of 2.39 eV is close to the 2.339 eV of GaP, and both gaps are indirect, with the conduction band minima at X .⁸ The static dielectric constants are similar, 9.7 for SiC¹⁸ and 10.75 for GaP.¹⁹ Carrier masses in SiC are not known, but are thought to be larger than those of GaP, hence SiC donor and acceptor ionization energies are likely to be larger. One of the more significant differences is that the lattice constant of cubic SiC, $a_0=4.36$ Å, is considerably smaller than the $a_0=5.45$ Å of GaP. A DA separation of 17 Å in a type-II spectrum occurs at shell $m=31$ in SiC, compared with $m=20$ in GaP. Thus, the "close pairs" part of a spectrum extends to somewhat larger m in SiC, and this region is often difficult to fit.

A. Fitting the Line Spectrum

We first used a table of shell substructure components and Eq. (1) to identify the line spectrum as type II, and to identify the shell numbers of as many lines as possible. A type-II spectrum results from donors on one sublattice and acceptors on the other. This is the expected type for N-Al pairs, for the N is on C sites, and the Al is on Si sites.

We next examined the spectrum for $m \geq 32$. There are two simplifying features for moderately large m : (1) Multipole splittings are small, and (2) the term E_{vdW} is proportional to r^{-6} . We rewrite Eq. (1), putting $E_{vdW} = -(e^2/\epsilon)(\alpha^5/r^6)$, where α is a positive constant, and we replace the constant terms $E_g - (E_D + E_A)$ by the single constant $h\nu_\infty$. Thus, we obtain

$$h\nu + E_C = h\nu_\infty - (e^2/\epsilon)(\alpha^5/r^6). \quad (4)$$

We calculated E_C for each shell m ,²⁰ using only the monopole term $E_C = -e^2/\epsilon r$, with $\epsilon=9.7$. Using the measured photon energies (averaged for each shell, if necessary), we then plotted the left-hand side of Eq. (4) against r^{-6} (Fig. 5). Thus, we obtained the intercept $h\nu_\infty=2.0934$ eV, and the van der Waals constant $\alpha=8$ Å (valid for large m).²¹ Some of the scatter in Fig. 5 is due to our neglect of the multipole terms. If the

plot of Fig. 5 is continued to $m < 30$ ($r < 17 \text{ \AA}$) the points deviate more and more from the straight line, indicating a failure of the r^{-6} dependence for E_{vdw} .

The static dielectric constant was found to be 9.72 at room temperature,¹⁸ but it has not been measured at the luminescence temperature of 1.8°K. In plotting Fig. 5 we tried several values of ϵ , and 9.7 appeared to give the best fit, but the plot is not very sensitive to changes of ± 0.1 in ϵ . For GaP the value of ϵ at 1.6°K is 3.3% smaller than at 300°K.¹⁹ The temperature dependence of ϵ appears to be considerably smaller in SiC than in GaP, which may be due to the fact that SiC has much larger phonon energies⁸ and direct band gaps.²²

The exciton energy gap of cubic SiC is known to be $E_{\text{gx}} = 2.39 \text{ eV}$.⁸ The energy gap appearing in Eq. (1) is the energy required to produce separated electron-hole pairs, $E_g = E_{\text{gx}} + E_x$, where E_x is the exciton binding energy. Thus, we find, for N-Al pairs, $E_D + E_A = 2.39 - 2.0934 + E_x = (297 \text{ meV}) + E_x$. It is difficult to obtain E_x from experiment. For Si, absorption measurements gave $E_x = 14.7 \text{ meV}$,²³ close to the effective mass value. For SiC, E_x is probably larger than for Si, but we will not attempt to estimate it.

Hall measurements have been made on N-doped cubic SiC,²⁴ but the data suggest that the samples were too heavily doped to yield the true value of E_D . Many measurements have been made on N-doped and Al-doped SiC of other polytypes, and it is found that $E_A \approx 2E_D$. If a similar ratio is valid for cubic SiC we can use our value of $E_A + E_D$ to make a rough estimate of $E_A \approx 200 \text{ meV}$ and $E_D \approx 100 \text{ meV}$. The same estimate of E_D is obtained by using Haynes rule²⁵ and the value $E_{4x} = 10 \text{ meV}$ for the energy binding an exciton to a neutral N atom.⁸ It is useful to have an order-of-magnitude estimate of E_A and E_D to aid in interpreting the intensity anomalies.

B. Intensity Anomalies

Two intensity anomalies can be observed in Fig. 3 by comparing heights of the lines marked "24." These are the lines to which the maximum number of 24 equivalent DA pairs contribute. There is an intensity cutoff between $m = 16$ and 15. The intensity reduction is about a factor 2, for only 12 pairs contribute to each of the $m = 16$ lines, but 24 pairs contribute to the single $m = 15$ line. The second anomaly is an enhancement by close to a factor 2 for $m = 11-8$. These lines stand out with respect to those on either side. The intensity ratios obtained from a densitometer trace are approximate, but a scan of the region using a photoelectric detector showed very nearly the same intensity ratios.

Keeping in mind the previous estimates of E_D and E_A , we find only one way to account for the anomalies. First, we attribute the cutoff between $m = 16$ and 15 to a closing of the $e-h$ capture channel, i.e., we conclude that the $e-h$ capture mode is energetically forbidden for $m \leq 15$. We then attribute the enhanced intensity in the interval $m = 11-8$ to the equality of E_{L2} and the LO

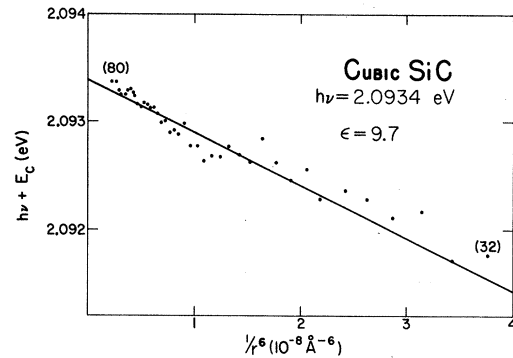


FIG. 5. Plot of $h\nu + E_C$ against r^{-6} for $32 \leq m \leq 80$, where $h\nu$ is the measured photon energy, and E_C is calculated with $\epsilon = 9.7$. The intercept at $r^{-6} = 0$ is $h\nu_{\infty} = 2.0934 \text{ eV}$, and the slope of the line is a measure of the van der Waals interaction.

phonon (120.5 meV), with capture necessarily through the $h-e$ channel. A rather broad resonance is not unexpected, for it depends on the slow change with m of the difference between the two small terms E_{pol} and E_{vdw} . The capture involved in both anomalies is electron capture by the N ion, first-capture in the cutoff, and second-capture in the resonance. Thus, for the cutoff, Eq. (2) is to be used as written, but, for the resonance, we must make the interchange required for the $h-e$ channel, so that Eq. (3) also contains E_D , not E_A .

In order to use Eqs. (2) and (3) we had to estimate E_{pol} . For this purpose we employed the values of E_{pol} deduced for S in GaP.⁷ The smaller dielectric constant of SiC and the larger E_D for N led us to take for $E_{\text{pol}}(\text{N})$ a bit less than the lower limit of the value found for S in GaP at the same DA separation. These are the values shown in the first two rows of Table I, the two rows that evaluate the limits placed on E_D by the cutoff anomaly.

For the resonance anomaly we must estimate $E_{\text{pol}}(\text{Al})$ even though E_D now enters Eq. (3), for in the initial state of second-capture the polarized atom is Al. Here the GaP work provides only a minimum of guidance, for the DA separation is small and Al is a fairly deep acceptor. Both factors require an extrapolation beyond the GaP data, one in the direction of increasing E_{pol} and the other in the direction of decreasing E_{pol} . However, the value $E_{\text{pol}} = 10.5 \text{ meV}$ shown in Table I is probably within a few meV of the correct value, and its substitution in Eq. (3) yields a value $E_D = 118 \text{ meV}$ that falls within the limits set by the cutoff anomaly.

We substitute $E_D = 118 \text{ meV}$ in the previously deduced expression for the sum of the ionization energies, $E_D + E_A = 297 \text{ meV} + E_x$. Thus, we obtain $E_A = 179 \text{ meV} + E_x$. The uncertainty in E_D and E_A is largely due to the uncertainty in E_{pol} .

C. Band Spectrum

Thomas *et al.* have given the theory of the DA band spectrum and have used it to interpret experiments on

TABLE I. Various energies, in meV, used to interpret the intensity anomalies. In the first two rows Eq. (2) is applied to the cutoff limits. In the third row Eq. (3) is applied to the phonon resonance.

Channel	Imposed condition	Shell m	$-E_C$	Estimated $-E_{\text{poi}}$	$-E_{\text{vdw}}$	Deduced E_D
$e-h$	$E_{L1}=0$	16	122.8	7.5		115.3
$e-h$	$E_{L1}=0$	15	127.0	8.0		119.0
$h-e$	$E_{L2}=120.5$	8-11		10.5	13.0	118.0

C-S pairs in GaP.²⁶ Our no-phonon band for N-Al pairs in SiC is well resolved, but we have too little information on saturation, impurity concentrations, and decay times for a detailed comparison with theory. However, Morgan *et al.*²⁷ have given relations between the band width and the band maximum that can easily be applied to our experimental results.

If we take the zero of the energy scale at $h\nu_\infty$ the energy of the band maximum is $E_{\text{max}} = -E_C(\text{max})$, for E_{vdw} is negligible at large m . For the band width at half-maximum Ref. 27 gives $\Delta E = 1.34E_{\text{max}}$ for saturated DA pairs, and $\Delta E = 0.76E_{\text{max}}$ for polyunsaturated pairs, i.e., for very low excitation intensity. The N-Al no-phonon band is shown in Fig. 4 for low and high excitation intensities. The peak energies $E_{\text{max}} = h\nu - 2.0934$ eV, are given in Table II, together with the corresponding shell numbers and DA separations. The experimental and theoretical band widths are also shown. For low intensity our measured band width is near the unsaturated limit. For high intensity it is approximately half-way between the two limits.

The impurity concentration N_i may determine the unsaturated band maximum, for recombination is less likely at DA separations much larger than the average interimpurity distance.²⁷ From $r = 58.4 \text{ \AA}$ we obtain $N_i = 1/\pi r^3 = 1.6 \times 10^{18} \text{ cm}^{-3}$, which is a reasonable value for either N or Al in our samples.

The second band system reported by Zanmarchi,¹¹ which he called "A," had a maximum at 2.155 eV independent of excitation intensity. He attributed the A system to Al, and derived a value of 235 meV + E_x for the Al ionization energy. However, this is 56 meV larger than we find for E_A from the DA line spectrum.

D. Multipole Moments

The charge distribution of the donor or acceptor ion has T_d point group symmetry, and can conveniently be expressed in lattice harmonics.²⁸ For the zinc-blende lattice the leading terms are third- and fourth-order harmonics, so the major part of the ion-ion interaction can be written

$$E_C = -e^2/\epsilon r + V_3 + V_4,$$

where

$$V_3 = k_3xyz/r^7$$

and

$$V_4 = k_4(x^4 + y^4 + z^4 - 0.6r^4)/r^9.$$

V_3 and V_4 are the multipole terms that give rise to separate spectral lines for each inequivalent set of DA pairs of a given shell, for these terms depend not only on the distance r , but also on the direction in the lattice from donor to acceptor.

The coefficients k_3 and k_4 can be evaluated by fitting the shell substructure lines of the spectrum, but a satisfactory fit has been made *only* for GaP DA spectra in which the donor is O and the acceptor is C,²⁹ Zn,⁶ or Cd.⁷ Because of the strong binding of the orbital electron to the O ion ($E_D = 895$ meV)¹⁹ the atom O has very little polarizability, and E_{vdw} is negligible in these spectra. In other DA spectra E_{vdw} is significant, and for close pairs it deviates strongly from an r^{-6} dependence. It seems probable that there is a directional dependence of E_{vdw} for close pairs. Then Eq. (1) shows that the directional terms of E_{vdw} would add to or subtract from the multipole terms of E_C .

An attempted multipole fit of several GaP spectra *not* having O as donor shows that the constants k_3 and k_4 fitted at large m are too large at small m . This failure, and the failure of the r^{-6} dependence of E_{vdw} occur at approximately the same value of m . Thus, the multipole moments evaluated at small m probably have contributions from both E_C and E_{vdw} , the latter having an unknown dependence on r .

There is also some difficulty in evaluating the multipole moments at large m , for then the shell substructure is often not well resolved. Nevertheless, it appears that only a fit in this region has significance for the determination of ionic charge distributions. For the N-Al

TABLE II. Band maximum and width under low and high excitation. All energies are in meV. The first three columns give the band maximum, the corresponding shell m , and the DA separation r . The last three columns give the measured band width ΔE , and the theoretical low and high excitation limits from Ref. 27.

	E_{max}	m	r (\AA)	ΔE	$0.76E_{\text{max}}$	$1.34E_{\text{max}}$
Low	25.4	360	58.4	19	19.3	34.0
High	33.4	210	44.4	35	25.4	44.7

pairs we fitted the region $30 < m < 44$ to obtain $k_3 = 2 \times 10^5 \text{ \AA}^4 \text{ meV}$, and $k_4 = 1.9 \times 10^6 \text{ \AA}^5 \text{ meV}$. These are composite values, with contributions from both N and Al ions.⁶ Even though these values of k_3 and k_4 do not fit the lines at small m , they do indicate the direction in which a shell component should be displaced, and they are therefore useful in making a complete identification of all the spectral lines.

The magnitudes of k_3 and k_4 for N-Al pairs in SiC are very similar to those found in the three fitted DA spectra of GaP. However, the lattice constant of SiC is smaller, so the multipole displacements are larger in SiC for equal m .

V. SUMMARY

A type-II DA pair spectrum in cubic SiC was recorded at 1.8°K, using laser excitation. The circumstances of crystal growth and the freedom from extraneous lines lead us to attribute the spectrum to the donor N on C sites and the acceptor Al on Si sites. Cubic SiC and GaP both have the zinc-blende lattice, hence the same DA shell structure. Many comparisons can therefore be made with the well-studied DA spectra in GaP. For example, the same table of shell substructure components can be used to identify the shell numbers. In the N-Al spectrum the lines are well resolved up to the 80th shell. Beyond that it is an easy extrapolation to infinite DA separation, which yields a value of $h\nu_\infty = 2.0934 \text{ eV}$. Knowing $E_{gx} = 2.39 \text{ eV}$, we obtain $E_D + E_A = 297 \text{ meV} + E_x$, where E_x is the still-unknown exciton binding energy.

The evaluation of E_D and E_A separately depends on

the interpretation of two intensity anomalies of the kind previously observed in GaP DA spectra. One anomaly is explained as the N first-capture cutoff, and the other is attributed to a coincidence between a capture energy E_{L2} and the LO phonon energy (120.5 meV). Thus, we find $E_D = 118 \text{ meV}$ for N, and $E_A = 179 \text{ meV} + E_x$ for Al.

The van der Waals energy was evaluated in the region $m > 30$, where it is proportional to r^{-6} . The multipole moments were also evaluated in this region. In cubic SiC, as in GaP, the difficulty in fitting multipole moments at small m appears to be related to the failure of the r^{-6} dependence of E_{vdw} at small m .

The relatively small lattice constant of SiC leads to large multipole terms at small m . This, and the intensity anomalies, made it difficult at first to identify the sharpest and best-resolved lines of the spectrum. A great help in the interpretation of these lines was provided by the solution of the problems of multipole moments and intensity anomalies in the GaP spectra.

Under lower resolution we observe only the envelope of the DA spectrum, which then appears to be a band spectrum with phonon replicas. From the replicas, phonon energies of 69, 94, and 118 meV are derived. The no-phonon band has the expected width and dependence on excitation intensity. From the peak position at low excitation we deduce an impurity level of $1.6 \times 10^{18} \text{ cm}^{-3}$.

ACKNOWLEDGMENTS

We wish to thank D. R. Hamilton for the crystals, and D. W. Feldman for the use of the Ar ion laser.

¹ J. J. Hopfield, D. G. Thomas, and M. Gershenzon, Phys. Rev. Letters **10**, 162 (1963).

² D. G. Thomas, M. Gershenzon, and F. A. Trumbore, Phys. Rev. **133**, A269 (1964).

³ F. A. Trumbore and D. G. Thomas, Phys. Rev. **137**, A1030 (1965).

⁴ P. J. Dean, C. H. Henry, and C. J. Frosch, Phys. Rev. **168**, 812 (1968).

⁵ P. J. Dean, C. J. Frosch, and C. H. Henry, J. Appl. Phys. **39**, 5631 (1968).

⁶ Lyle Patrick, Phys. Rev. **180**, 794 (1969).

⁷ P. J. Dean and Lyle Patrick, Phys. Rev. B **2**, 1888 (1970).

⁸ W. J. Choyke, D. R. Hamilton, and Lyle Patrick, Phys. Rev. **133**, A1163 (1964).

⁹ M. Lax, Phys. Rev. **119**, 1502 (1960).

¹⁰ The criterion for capture may be written $E_{Li} > \frac{3}{2}kT$, as in Ref. 9, but $\frac{3}{2}kT$ is negligible at 1.8°K.

¹¹ G. Zanmarchi, J. Phys. Chem. Solids **29**, 1727 (1968).

¹² D. R. Hamilton, J. Electrochem. Soc. **105**, 735 (1958).

¹³ W. J. Choyke, Mater. Res. Bull. **4**, S141 (1969).

¹⁴ R. L. Hartman and P. J. Dean, Phys. Rev. B **2**, 951 (1970). Hartman and Dean show that the spectrum is due to an exciton bound to a donor.

¹⁵ The shell substructure is identical with that of a type-II GaP spectrum. No extensive list of the component sets has been

published. Table I of Ref. 6 identifies the inequivalent sets for shells $8 < m < 18$.

¹⁶ The absence of extraneous lines would be difficult to explain if the spectrum were attributed to pairs other than N and Al.

¹⁷ D. W. Feldman, James H. Parker, Jr., W. J. Choyke, and Lyle Patrick, Phys. Rev. **173**, 787 (1968).

¹⁸ Lyle Patrick and W. J. Choyke, Phys. Rev. B **2**, 2255 (1970).

¹⁹ Lyle Patrick and P. J. Dean, Phys. Rev. **188**, 1254 (1969).

²⁰ The relation between r and m , as given in Ref. 1, is $r = (8m - 5)^{1/2} a_0/4$, with $a_0 = 4.36 \text{ \AA}$ for cubic SiC.

²¹ The value derived for the van der Waals constant α is quite sensitive to the value of ϵ used to calculate E_C in Eq. (4).

²² W. J. Choyke and Lyle Patrick, Phys. Rev. **187**, 1041 (1969).

²³ K. L. Shaklee and R. E. Nahory, Phys. Rev. Letters **24**, 942 (1970).

²⁴ A. Rosengreen, Mater. Res. Bull. **4**, S355 (1969).

²⁵ J. R. Haynes, Phys. Rev. Letters **4**, 361 (1960). For Si, Haynes found $E_{4z} \approx 0.1 E_D$.

²⁶ D. G. Thomas, J. J. Hopfield, and W. M. Augustyniak, Phys. Rev. **140**, A202 (1965). The DA spectrum was attributed to Si-S pairs, but was later shown to be due to C-S (Ref. 5).

²⁷ T. N. Morgan, T. S. Plaskett, and G. D. Pettit, Phys. Rev. **180**, 845 (1969).

²⁸ D. G. Bell, Rev. Mod. Phys. **26**, 311 (1954).

²⁹ Lyle Patrick, Phys. Rev. Letters **21**, 1685 (1968).